Biochemical Engineering Journal 159 (2020) 107624

Contents lists available at ScienceDirect

Biochemical Engineering Journal

journal homepage: www.elsevier.com/locate/bej

Regular article

Identifying metabolic features and engineering targets for productivity improvement in CHO cells by integrated transcriptomics and genome-scale metabolic model

Zhuangrong Huang, Seongkyu Yoon*

Department of Chemical Engineering, University of Massachusetts Lowell, Lowell, MA 01854, USA

HIGHLIGHTS

- Transcriptomics analysis was used to study metabolism change over the batch culture.
- Metabolic pathway alternations were analyzed between high and low producers.
- Key pathways related to productivity increase and high productivity were elucidated.
- Combined transcriptomics and flux analysis allow to identify metabolic bottlenecks.

ARTICLE INFO

Keywords:
Metabolic pathway analysis
Genome-scale metabolic model
Chinese hamster ovary
Flux balance analysis
mAb productivity

ABSTRACT

In this study, we presented an integrated systems biology approach to elucidate the key characteristics of cellular metabolism in Chinese hamster ovary (CHO) cells producing monoclonal antibodies (mAb). The cellular metabolism in high and low producers under batch conditions was interrogated dynamically both within and among cells. First, transcriptomics analysis was used to study the time-course change in the metabolic pathway within cells that was correlated with mAb productivity increase. Second, differentially regulated pathways between high and low producers were sought at each growth phase. Several up-regulated pathways were identified in the high producer at the late growth phase, including citrate cycle, oxidative phosphorylation, and pentose phosphate pathway. These activities were further analyzed by intracellular flux distributions estimated through a genome-scale CHO model. Our results revealed that these key pathways are identified to be characteristics of high mAb production, not only for the high-producing cell line but also a dynamic phenomenon in mAb-producing cell cultures. This study showed that the approach of integrating transcriptomics and flux analysis leads to a better understanding of cellular metabolism related to mAb productivity. In turn, this allows for the identification of metabolic bottlenecks and potential engineering targets for cell line development and process optimization.

1. Introduction

Chinese hamster ovary (CHO) cells are the predominant mammalian host for therapeutic monoclonal antibodies (mAb) production. The product yield in CHO cells has increased more than 100-fold over the past several decades [1,2]. Much of this progress has been achieved through experimental approaches including media and feeding strategies, and process condition optimization [3–7]. Improved understanding of cellular metabolism in CHO cells continues to accelerate rational cell line development and bioprocess optimization towards cell growth or mAb production [8–10].

High-throughput omics data analysis for CHO cells have been recently conducted [11–13]. Studies have explored the links between gene expression and high productivity by the effect of temperature downshift [14,15], autophagy inhibitor 3-methyladenine treatment [16], and inducer treatment [15,17]. Similarly, proteomic-based techniques were applied to distinguish enzyme expression differences between high and low producers [3,18]. Metabolomics based on liquid chromatography-mass spectrometry (LC-MS) has also been used to explore the relationship between metabolite levels and high mAb productivity [19].

While individual omics technologies can provide insights into the

* Corresponding author at: 1 University Ave, Lowell MA 01854, USA.
E-mail address: Seongkyu_Yoon@uml.edu (S. Yoon).

https://doi.org/10.1016/j.bej.2020.107624
Received 26 December 2019; Received in revised form 21 April 2020; Accepted 27 April 2020
Available online 05 May 2020
1369-703X/

cellular metabolism, these omics are closely interconnected and should be viewed by integration to study the biological system comprehensively [20]. For example, gene expression levels may not always correlate to protein regulation [21]. Similarly, protein expression alone does not necessarily correlate with the change in enzymatic activity [1]. Therefore, combined omics approaches are needed to build connections between phenotype and genotype and to provide a more comprehensive understanding of cell physiology [22]. In this regard, the genome-scale network of CHO metabolism offers an effective tool for integrating omics data and metabolism understanding. This has been well demonstrated by several previous studies. For example, Hefzi et al. have applied omic data to reveal an amino acid auxotrophies in different CHO cell lines [23]. Yusufi et al. used the integration of transcriptomic data with a genome-scale model, to find out that the antibody producer has a substantial increase in energy metabolism than the wild-type CHO cell [8]; subsequently, a study conducted by the same group unraveled cell line-specific variations in protein processing abilities and glycosylation profiles across different CHO host cell lines (including CHO-K1, CHO-DXB11, and CHO-DG44) [24]. Recently, Vodopivec et al. applied the genome-scale metabolic model to analyze the metabolomics data at different fed-batch bioreactor scales (10L, 100L, and 1000L) and gained insight into the metabolic states [25].

Cell dynamics are critical to the phenotypes of cell growth and mAb production. To our knowledge, there has been no research reported to investigate whether high-producing CHO cells would exhibit a different metabolic characteristic (on metabolic pathway) than those with low productivity in response to the growth phase transition. Current advances in transcriptomics analysis allow us to reveal and quantify biological processes in CHO cells [13,24,26]. Gene expression profiles can demonstrate which genes are active and allow us to deduce the corresponding pathways utilized in cellular metabolism. Additionally, changes in gene expression levels between culture conditions or cell lines with different productivities may help in identifying which pathways are differentially regulated that could be potential targets for improvement of mAb production. While gene expression profiles provide insights into transcriptional patterns, intracellular metabolic flux describing the metabolic activity within the cell represents another informative attribute of the cellular state.

Our objective was to apply transcriptomics, together with extracellular metabolomics and a genome-scale metabolic model to decipher the cellular metabolism in order to expand the understanding of which metabolic pathways play a critical role in mAb production. To achieve this, we applied a systems biology approach with a particular focus on metabolic pathway analysis using two CHO cell lines displaying different mAb productivities. In this study, we first used transcriptomics to screen for metabolic alteration during the course of cell culture. Metabolic changes relevant to different productivity increases were identified by the unique dynamic pattern of pathway regulation present in either the high- or low-producing cell line. To obtain orthogonal information, the characteristics of high productivity were further explored using metabolic pathway analysis from each culture stage between high- and low-producing cell lines. A genome-scale metabolic model was then used to estimate the intracellular fluxes and enable an analysis of cellular metabolism from the perspective of reaction rates. As such, the combined studies of transcriptomics and flux analysis have converged on the key characteristics of high-producing CHO cells, which allows us to identify metabolic bottlenecks and potential engineering targets for cell line development and process optimization.

2. Materials and methods

2.1. Cell culture experiments and measurements

Two glutamine synthetase (GS) CHO cell lines CHO-A and CHO-R producing different mAbs were used in the study and termed high producer (HP) and low producer (LP), respectively. The detailed information on cell culture experiments can be found in the previous publication [13]. Cells were cultured in commercial media CD FortiCHO (ThermoFisher Scientific, Waltham, MA) with an inoculation density of 2×10^5 cells/mL and a working volume of 50 mL in shake flasks. For each cell line, triplicate flasks were cultured for seven days in batch mode. Gene expression profiles were determined using RNA-sequencing (RNA-Seq) at day 3 and day 6, which corresponded to the early and late exponential growth phase, respectively. All transcriptomes were normalized as TPM (transcripts per million). Metabolic genes for CHO cells were found in the published genome-scale CHO model [23] or BIGG database (http://bigg.ucsd.edu). Wilcoxon rank sum test, which is a nonparametric test without the assumption of certain distribution, was implemented to evaluate the gene expression profiles under different conditions [27–30]. The main idea of this test is the ranks of the observations are used as test statistics instead of the original gene expression values when comparing the gene expressions between two independent groups.

The concentration of amino acids was measured using a HPLC system (Shimadzu, Kyoto, Japan) connected with a triple quadrupole mass spectrometer (Shimadzu, Kyoto, Japan) operated in positive electrospray ionization mode. A column Scherzo SM-C18 (3 μm, 100 × 3 mm, IMTAKT) was used for the component separation. Amino acid standard mixtures were separated using an Intrada Amino Acid column (100 × 3 mm, 3 μm, IMTAKT, Japan). Mobile phase A (aqueous) consisted of 0.3% v/v formic acid in acetonitrile and mobile phase B (organic) consisted of 20% v/v acetonitrile in 100 mM ammonium formate. The chromatographic separation was accomplished by different gradients of aqueous and organic phase as follows: the mobile phase was started at 20% B for 4 min, increased from 20% B to 100% B with a linear gradient for 10 min, then maintained at 100% B for 2 min. The mobile phase was returned to 20% B and continued for 2 min. LC conditions included column temperature at 37 °C, injection volume of 10 μL, and mobile phase flow rate of 0.6 mL/min. More detailed information about the quantification of amino acids by LC–MS/MS can be found as previously described [31].

2.2. Metabolic pathway analysis

Metabolic gene expression levels were considered different when their fold change (i.e., the relative change in gene expression compared to control) was at least 1.3 and p-value calculated from these two datasets via ANOVA (Analysis of variance) should be less than 0.05. It is important to note that the threshold is user-defined. In previous studies, different fold-changes from 1.2 to 1.5 or higher have been used [13,32–34]. KOBAS 3.0 was used to perform the pathway enrichment analysis using identified differentially expressed genes (DEGs) [35]. In statistics, the p-value of a particular pathway was calculated using the hypergeometric test/Fisher's exact test as follows:

$$p = 1 - \sum_{i=0}^{m-1} \frac{\binom{M}{i}\binom{N-M}{n-i}}{\binom{N}{n}} \quad (1)$$

where N is the total number of genes mapped to all annotated pathways in CHO cells; n is the total number of differentially expressed genes; M is the total number of genes in the particular pathway under investigation; m is the number of differentially expressed genes in the particular pathway [36–39]. In KOBAS 3.0, the resulting p-values in enrichment analysis were adjusted for multiple testing using the Benjamini-Hochberg method [40]. In this analysis, the pathways with adjusted p-value < 0.05 were considered as significantly enriched. The Kyoto Encyclopedia of Genes and Genomes (KEGG) pathway database of Cricetulus griseus (Chinese hamster) was employed during the analysis (https://www.genome.jp/kegg/).

2.3. Flux balance analysis using the genome-scale model

A recently published genome-scale CHO-S model was applied to analyze the metabolism of CHO cells in this study [23]. Intracellular metabolic fluxes were estimated by flux balance analysis (FBA) with the optimization of a defined biological objective function using a linear programming approach. The genome-scale model can be represented by a stoichiometric matrix (S) of size m× n (where m represents the number of metabolites and n represents the number of reactions, respectively) and a vector of reaction fluxes (v) [41–43]. The mass balance equations are given by S× V= 0 under the assumption of quasi-steady-state. To obtain the solution, the genome-scale model was further constrained by the boundaries of each flux. The value of the upper bound was set to 1000 for all reactions; the value of the lower bound was set to −1000 or 0 for reversible reactions and irreversible reactions, respectively [23]. For this work, parsimonious enzyme usage FBA (pFBA), which is a variant of FBA, was used for flux estimation [44]. This approach assumes that cells attempt to achieve optimal growth with the most efficient allocation of resources (i.e., minimization of enzyme usage) [45]. Therefore, a dual objective function, which is a combination of maximizing growth rate and minimizing overall flux, was applied to solve the flux distribution during the early and late exponential growth phases in this study. The Constraint-Based Reconstruction and Analysis (COBRA) toolbox was used for FBA analysis in this study [46,47]. Gurobi solver (https://www.gurobi.com/) was applied to solve LP optimization problems. MATLAB (Matlab 2016a; Mathworks, Natick, MA, USA) was used for the Wilcoxon test, ANOVA, and FBA in this study.

The uptake and secretion rates of metabolites (i.e., amino acids, glucose, lactate, ammonium) were calculated from measured time-series extracellular metabolomics by using the following equations (Eqs. 2–4).

$$dX/dt = \mu X \tag{2}$$

$$dP/dt = q_p X \tag{3}$$

$$dN/dt = -q_N X \tag{4}$$

where X, P, N, t are the viable cell density (VCD), product (e.g., lactate, ammonium, mAb, or other by-products in the supernatant), nutrient concentration (e.g., glucose, glutamate, and other amino acids) and time, respectively. The μ, q_p, and q_N represent the specific cell growth rate, secretion, and uptake rate of the extracellular metabolites, respectively. These specific metabolic rates were served as experimental metabolic constraints in genome-scale models. The metabolic models and the RNA-Seq data used in this study can be available by contacting the authors.

3. Results and discussion

3.1. Cell growth and mAb production

To ensure that cell line is the only factor on altering cellular metabolism, we cultured two cell lines HP and LP in batch shake flasks using the same media and culture conditions. Cell growth and mAb production profiles are shown in Fig. 1**A** and B, respectively. As seen, these two cell cultures revealed similar cell growth but distinct titer production profiles. The specific mAb productivity was calculated (as described in Materials and methods) and shown in Fig. 1**C** and D, respectively. Significant changes were observed along both the time course and between the two cell lines. First, from a dynamic point of view, the mAb productivity of HP had a substantial increase from the early to the late exponential growth phase, whereas LP only had little increase. Thus, there might be a metabolic transition correlated with the dynamic production of mAb, which would be different in the high- and low-producing cell cultures. Second, HP showed higher specific productivity at any growth phase compared to LP, for example, the productivity was 18-fold greater in HP compared to LP on day 6 (late growth phase) (Fig. 1**C** and D). This result points out that there can be another metabolic distinction just correlated between the two cell lines. In the following analyses, we assigned the day 3 to be an early growth stage and day 6 to be a late stage.

3.2. Overview of gene expression

We then analyzed the gene expression profiles of RNA-Seq data at the early and late growth phases (as shown in Fig. 2A). Out of 26,520 genes found in the global RNA-Seq data, we focused on the metabolic genes presented in the published genome-scale CHO model [23]. Our analyses were carried out in two orthogonal ways **(**Fig. 2**B** and C**)**. First, we defined the metabolic difference responsible for mAb productivity increase over the course of batch culture (Fig. 2B**)**. The process was by comparing the gene expression between early and late growth phases in HP to identify the differentially regulated pathways, and the same process was repeated in LP. Second, we investigated the metabolism difference at each growth phase between HP and LP (Fig. 2C). This was by comparing the gene expression between HP and LP at the early growth phase to identify the significantly changed pathways, and the same process was also performed for the late phase. Both aspects were aimed to identify the metabolic features that potentially contribute to high mAb productivity.

Fig. 3**A** shows the results of the Wilcoxon test. Any two states seeing a significant difference in the transcriptional levels are marked with asterisks. For the first goal, the Wilcoxon test revealed significant alteration at the transcriptomic level between early and late growth phases (p-value < 0.001 in the comparison of Early_HP and Late_HP; p-value < 0.01 in the comparison of Early_LP and Late_LP, as seen in Fig. 3A). Fig. 3B shows the number of DEGs between every two states. With a fold change > 1.3, a total of 114 DEGs across culture phases could be identified in HP (1st bars in Fig. 3B) and 107 DEGs in LP cultures (2nd bars in Fig. 3B). Taking the early phase as the control, 71 (60.7%) DEGs in HP cultures were up-regulated and 43 (39.3%) were down-regulated. Similarly, 57 (53.3%) DEGs in LP cultures were up-regulated and 50 (46.7%) were down-regulated. However, these numbers of DEGs that found to vary in the culture progression are less than 9% of the total 1273 metabolic genes in the genome-scale CHO-S metabolic network, indicating that the overall transcriptome was stable during the course of culture.

Next, we analyzed the gene expression difference between HP and LP cultures. The Wilcoxon test results in Fig. 3**A** show that the HP and LP cultures have no significant difference at the early growth phase (p-value > 0.05 in the comparison of Early_HP and Early_LP, as seen in Fig. 3A). Consistently seen with the number of DEGs (3rd bars in Fig. 3B), at the early growth phase, only four genes were more expressed in HP compared to LP cultures and two genes were less expressed. In contrast, the Wilcoxon test indicated that genes were distinctively expressed at the late growth phase between HP and LP cultures (p-value < 0.001 in the comparison of Late_HP and Late_LP, as seen in Fig. 3A). A total of forty-one metabolic genes were more expressed in HP, while only two genes were less expressed (4th bars in Fig. 3B).

3.3. Metabolic pathway analysis between early and late growth phases

Here, the identified DEGs along the culture progression were further interrogated by metabolic pathway analysis. The DEGs between early and late growth phases were projected to the KEGG pathway database. Fig. 4 gives an overview of the metabolic pathways identified as up- or down-regulated at the late growth phase compared to the early phase (up-regulated shown in Fig. 4A and B; down-regulated shown in Fig. 4C and D). At first sight, the HP and LP cultures had many overlapped pathways (in gray, Fig. 4). This majority of similarity could be for the

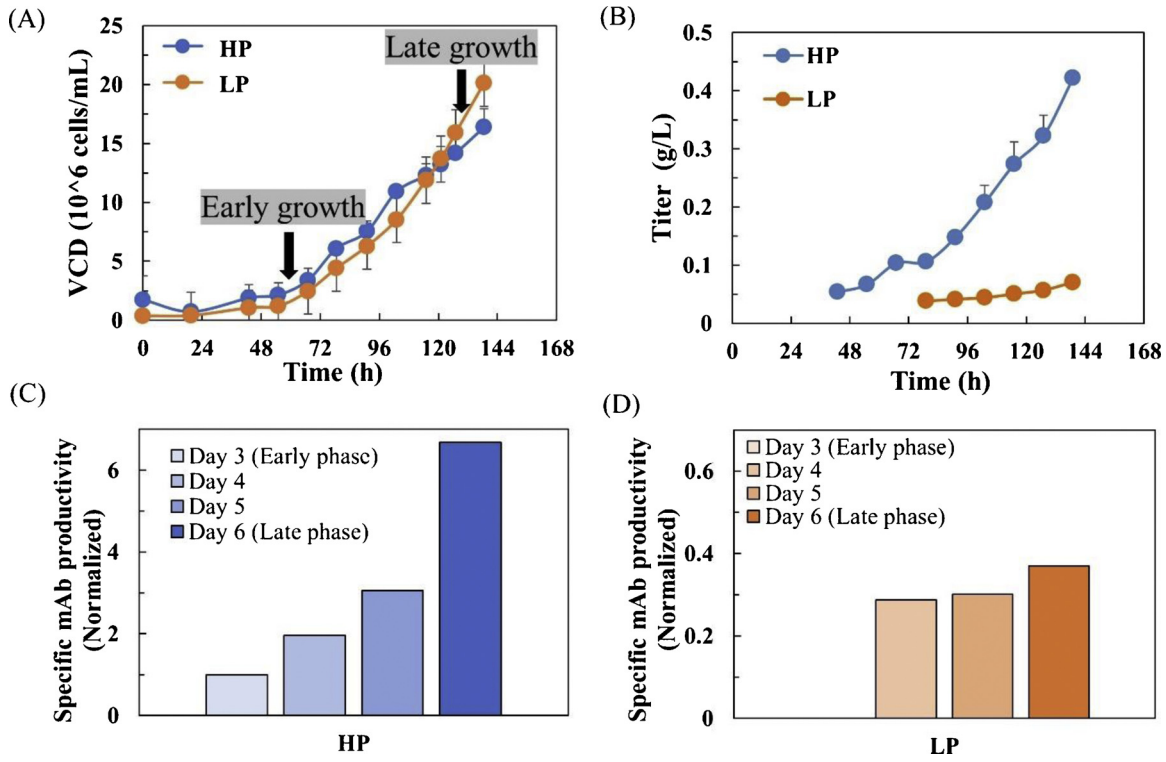

Fig. 1. Cell culture experimental data in HP (high producer) and LP (low producer) cultures. (A) Time-series viable cell density. (B) Time-series mAb production. (C) Specific mAb productivity in HP cultures. (D) Specific mAb productivity in LP cultures. The titer of LP at day 3 was close to zero, so the bar was not shown. The specific mAb productivity of the early phase in HP was set as 100% to normalize productivity in figure C&D.

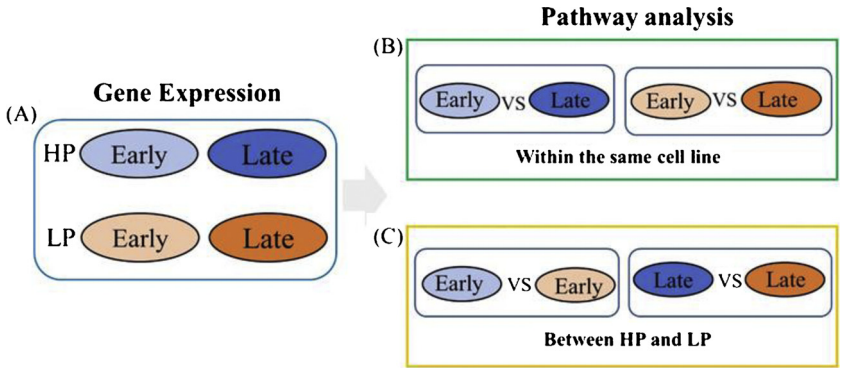

Fig. 2. Schematic overview of the comparative transcriptomics analysis between HP and LP.

general responses of cells in batch culture. To identify the pathways that may be uniquely associated with mAb productivity increase, we focused on the metabolic pathways that differed between HP and LP (in bold, Fig. 4).

Two pathways of glycan related metabolism (glycosaminoglycan biosynthesis, mucin type O-glycan biosynthesis) were up-regulated in HP at the late growth phase (Fig. 4A). This observation may indicate complex alternations in the normal physiological function of cells. However, this pathway is not directly associated with cellular metabolism that relates to cell growth and mAb production. The two pathways uniquely up-regulated in LP are alanine, aspartate and glutamate metabolism; and glycine, serine and threonine metabolism (Fig. 4B). The DEGs associated with this pathway are *Gamt*, *Sdsl*, *Sds*, *Gpt2*, *Asns*. To closely examine the expression of these genes, we plotted their expression data in Fig. 5. It turned out, these genes also underwent significant alteration during the progression of high-producing cells, except for the gene *Sdsl*. Whereas, the fold change of several genes in the high-producing cell culture was less than the 1.3, which was the cut-off threshold used for the DEGs identification. This explained why not all these genes were initially recognized as DEGs in the high-producing cell culture. In the meantime, it points out that these pathways were not the most distinct pathways that could be found between HP and LP cultures.

The same analysis was repeated on down-regulated pathways. It was observed that pentose phosphate pathway (PPP), citrate cycle (TCA cycle), cysteine and methionine metabolism were uniquely down-regulated in LP, suggesting that these pathways may be associated with the lower productivity increase in LP.

3.4. Metabolic pathway analysis between high and low producers

Metabolic pathway analysis was then carried out to distinguish activities altered between HP and LP cultures. Interestingly, the early growth phase witnessed little gene expression difference between HP and LP. Only six DEGs were found in total between the two cultures. In contrast, a significant change was observed at the late growth phase.

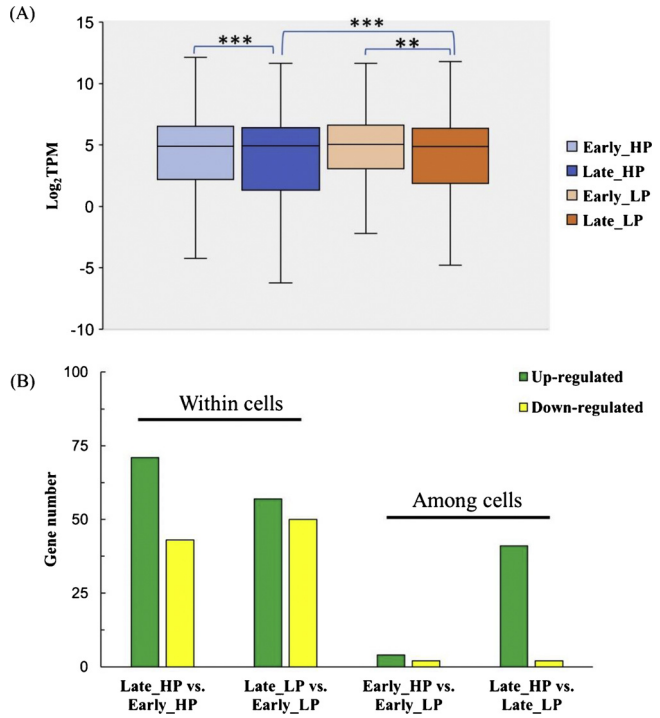

Fig. 3. Gene expression analysis comparing early and late growth phases and between HP and LP cultures. (A) Wilcoxon test. In boxplots, the centerline indicates the median, the box limits indicate the upper and lower quartiles, and the whiskers extend from the minimum to the maximum values. Statistical significance is indicated by asterisks according to the calculated p-values (*p-value < 0.05, **p-value < 0.01, ***p-value < 0.001). (B) The number of differentially expressed genes.

The pathways expressed significantly higher in HP cultures are listed in Fig. 6, including various lipid-related metabolism, energy-related metabolism, protein export, biosynthesis of amino acids, PPP, and amino sugar and nucleotide sugar metabolism.

Previous work has found that early cell culture has higher glycolytic activity in order to generate the required energy for cell growth [48]. However, during the late growth phase or mAb production phase, the energy is primarily provided through a stage called mitochondrial oxidative phosphorylation, which is associated with elevated PPP activity [49]. It is also conceivable that high productive cell lines enhance their mitochondrial function (TCA cycle) and up-regulate oxidative phosphorylation to ensure the increased generation of adenosine triphosphate (ATP) required for mAb production and redox needs [50]. The cellular activities found in our study for HP cultures at the late stage are consistent with these previous studies, suggesting that oxidative phosphorylation may play a vital role in mAb production.

PPP is a major source for generating NADPH which is the main intracellular reductant that can counteract oxidative damage. PPP also plays a vital role in the redox regulation, lipid synthesis, and regeneration of reduced glutathione [51,52]. In this study, PPP is significantly enriched at the late stage in HP deduced from gene expression analysis, which implies that PPP may play a critical role in the cellular redox state for mAb production.

3.5. Flux balance analysis with a genome-scale CHO model

After the transcriptomics analysis, we performed a flux balance analysis as another independent investigation between HP and LP. Since very similar key pathways were identified in Section 3.3 and Section 3.4, hence, we only discussed the flux analysis for Section 3.4 at the late growth phase where the largest metabolic difference was observed in terms of mAb productivity between HP and LP. Glycolysis, PPP, pyruvate catabolism, TCA cycle are the central metabolism for cell

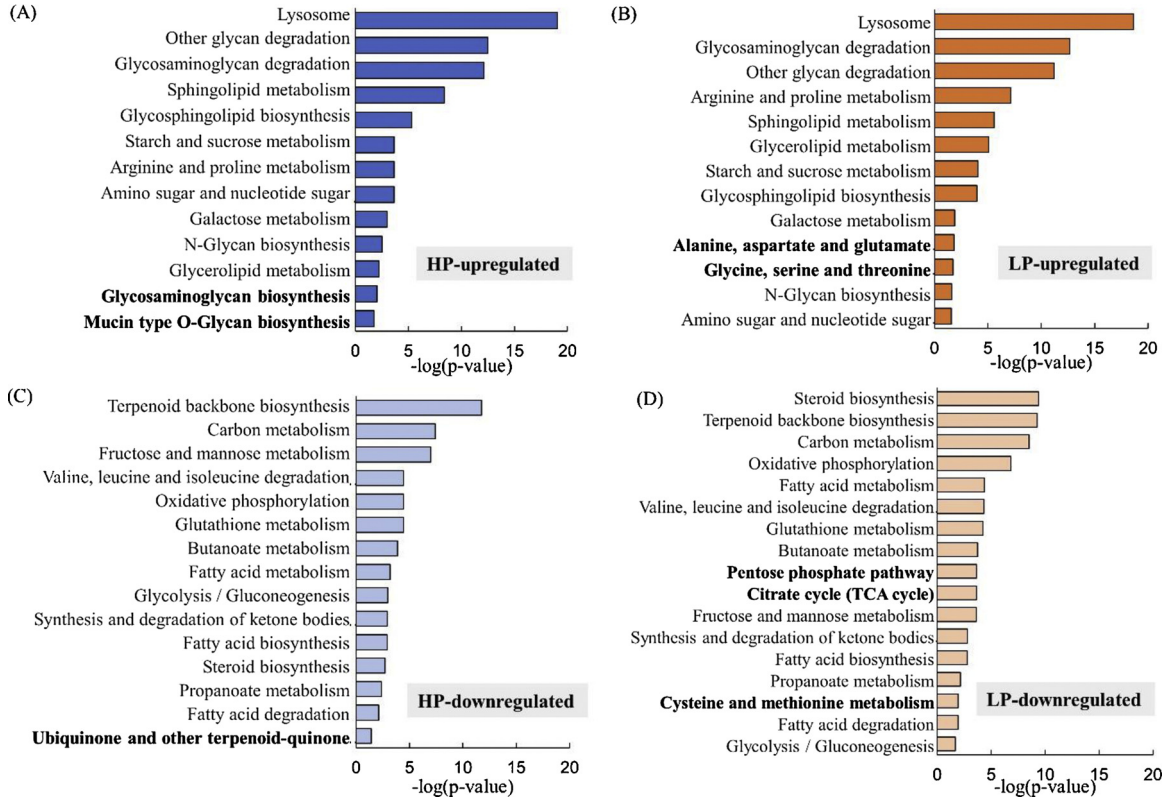

Fig. 4. Summary of the main results for the KEGG pathway analysis of transcriptomics. Pathways are up-regulated at the late growth phase compared to the early phase in HP (A) and LP (B); pathways are down-regulated at the late growth phase compared to the early phase in HP (C) and LP (D). All the pathways shown in the figure have achieved a significance value of non-log scale p-value < 0.05 (equivalent to a score higher than 1.3 on the *x*-axis).

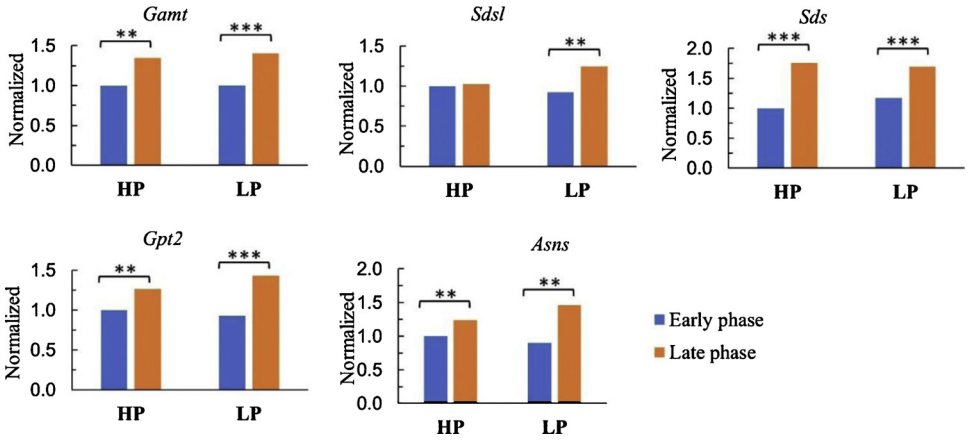

Fig. 5. Gene expression levels of identified DEGs involved in alanine, aspartate and glutamate metabolism, glycine, serine and threonine metabolism in HP and LP. Statistical significance is indicated by asterisks (* p-value < 0.05, ** p-value < 0.01, *** p-value < 0.001).

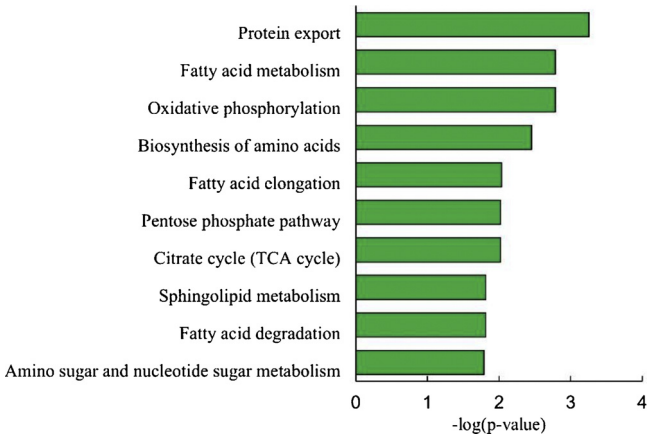

Fig. 6. Up-regulated pathways at the late growth phase in HP compared to LP. All the pathways shown in the figure have achieved a significance value of non-log scale p-value < 0.05 (equivalent to a score greater than 1.3 on the *x*-axis).

growth and mAb production (as shown in Fig. 7A). For each reaction, only the gene that differentially expressed between HP and LP (first-choice) or with the highest expression level (second-choice) at the late growth phase was shown in the figure at the side of metabolic reaction. A genome-scale metabolic model was applied to obtain the fluxes of these reactions, while the extracellular metabolite uptake and excretion rates calculated from experimental measurements were used as constraints in the model. Metabolic fluxes of these reactions calculated for the late exponential growth phase in HP and LP are shown in Fig. 7B. Below, the transcriptomics and metabolic fluxes indications of these reactions are discussed separately for the glycolysis and PPP pathways (Section 3.5.1) and the TCA cycle (Section 3.5.2). For convenience, in this article, the reactions and associated genes shared the same names but only the genes were presented in italic type.

3.5.1. Fluxes in glycolysis and pentose phosphate pathway

According to the transcriptomics analysis, PPP and TCA cycle are the two most significantly up-regulated central carbon metabolism at the late growth phase of HP. Hexokinase (HK) catalyzes the first step of glucose metabolism, phosphorylating glucose to glucose 6-phosphate (Glucose-6P). Both the *HK* gene expression and the flux of the HK reaction revealed that there was no big difference in HK activity between the two cultures. In the reactions of glyceraldehyde 3 phosphate dehydrogenase (GAPD) and phosphoglycerate kinase (PGK) in glycolysis, the predicted fluxes between HP and LP cultures are consistent with gene expression. It was found that fructose 6-phosphate (Fructose-6P) was converted to glucose-6P via the reaction of GPI according to predicted flux distribution in HP cultures, implying that PPP may be operating in a cyclic mode. While the predicted flux in the reaction of GPI was zero in LP culture. This is also possible as seen in predicted flux distribution in Fig. 7 that almost all of the transported glucose was consumed by diverting to PPP during the late exponential growth phase in LP cultures, and then went back to glycolysis through non-oxidative PPP (e.g., TKT (transketolase)). Overall, our flux distribution results are consistent with other studies where similar results were observed during the late growth stage [48].

An important gene in the PPP is glucose-6-phosphate dehydrogenase *(G6pd)* which coding the reaction of G6PD in mammalian cells to maintain the NADPH level. Given that G6PD is used in the first step of the PPP and always rate-limiting, there has been genetic engineering that overexpressed the genes in G6PD to improve protein production [53]. While our study did not observe a big difference in the gene expression of *G6pd* during the late growth phase between HP and LP cultures, instead, we found a significantly higher expression level in HP cultures on downstream genes in the PPP, including *Prps1* and *Prps2*. These genes are responsible to convert ribose-5-phosphate (R5P) into 5-phosphoribosyl-1-pyrophosphate (PRPP), which are probably a driving force for the higher activity of oxidative PPP in HP than LP cultures as observed in predicted flux distribution in Fig. 7.

3.5.2. Fluxes in the TCA cycle

It has been known that the majority of glycolytic-derived pyruvate was processed through the TCA cycle for energy generation when cells are not producing a large amount of lactate (e.g., during the late exponential growth phase or stationary phase of cell culture) [54]. The pyruvate dehydrogenase (PDH) plays a key role in linking glycolysis to the TCA cycle by converting pyruvate to acetyl-CoA. Our results showed that higher activity of PDH at both flux and gene expression levels in HP cultures. It is interesting to note that the activity of the TCA cycle is higher only for the lower part of the TCA cycle in HP, such as oxoglutarate dehydrogenase (ODH), succinyl-CoA synthetase (SUCOAS), succinate dehydrogenase (SDH), and malate dehydrogenase (MDH)). It was observed on both the gene expression and the predicted fluxes in HP cultures as seen in Fig. 7B. While upper TCA cycle appeared to have little difference in terms of both the predicted fluxes and gene expression between HP and LP cultures, such as citrate synthase (CS) and isocitrate dehydrogenase (IDH) as seen in Fig. 7B.

Among them, the most outstanding gene in the TCA cycle was *SUCOAS*, which catalyzes the reversible synthesis of succinate and ATP (Fig. 7**B**). Both gene expression and flux levels were higher in HP cultures, suggesting that the reaction of SUCOAS may be a metabolic bottleneck of the TCA cycle for mAb production. From literature, it has

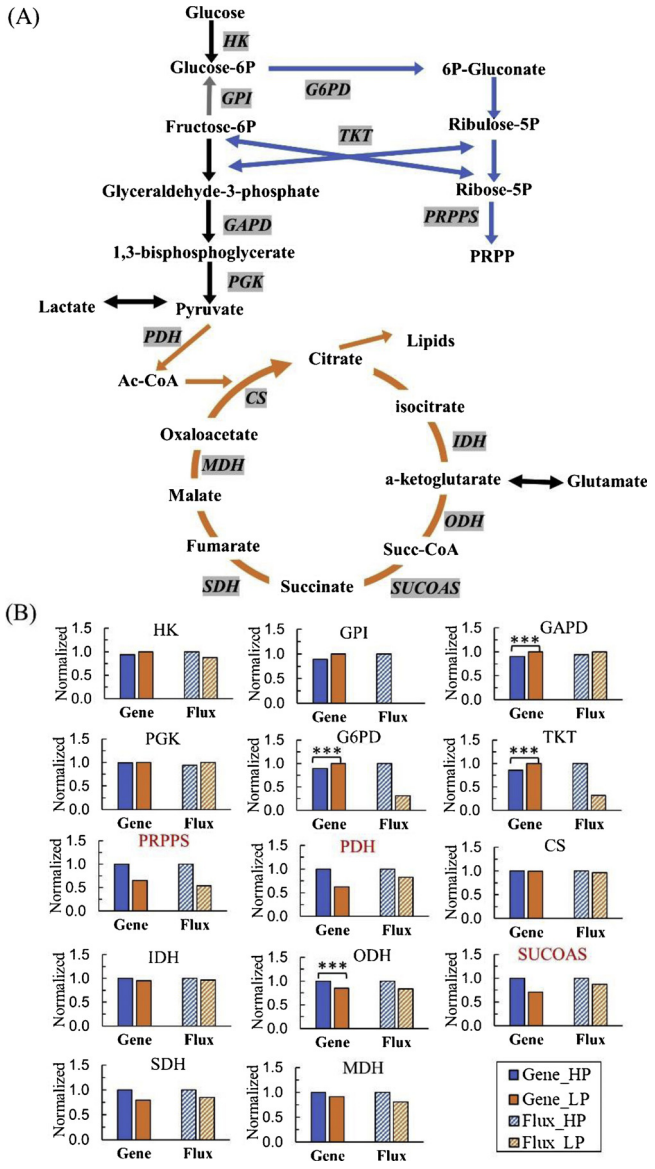

Fig. 7. Visualization of the gene expression levels and predicted reaction rates in selected key pathways (glycolysis, pentose phosphate pathway, and TCA cycle). The data including the gene expression levels and predicted reaction rates are normalized to the highest values for each reaction. The reactions regulated by DEGs are indicated in red. Statistical significance is indicated by asterisks (* p-value < 0.05, ** p-value < 0.01, *** p-value < 0.001) (For interpretation of the references to colour in this figure legend, the reader is referred to the web version of this article).

been reported that transient silencing of gene *Sucla2* which regulates SUCOAS would inhibit cell growth and decreased ATP production [55].

3.6. Summarization for the combined transcriptomics and flux analysis

In this study, we explored the metabolic differences between low- and high-producing cell cultures to identify potential targets for cell line development and bioprocess optimization. To this end, we combined transcriptomics and flux analysis through genome-scale CHO models. No significant phenotypic differences in viable cell density and viability were shown between the two cultures investigated. As a result of this, it allows us to focus on investigating the metabolic alternations related to productivity rather than considering the confounding effects of cell growth and its broad cellular consequences.

Firstly, it was found that both HP and LP showed a consistently elevated activity of mAb production over cell culture. Our primary interest here was to determine how cellular metabolism adapts to batch culture conditions and accordingly to identify the metabolic differences between HP and LP that may result in productivity discrepancy. Thus, the comparison of the transcriptome between early (with lower mAb productivity) and late (with higher mAb productivity) growth phases provides a view of metabolic responses to dynamic cell culture conditions. We observed that the vast majority of pathways gave the same responses to HP and LP favors common responses that may be associated with growth arrest and nutrient availability in the batch culture conditions. We also found that PPP, TCA cycle, cysteine and methionine metabolism were only down-regulated in LP cultures, suggesting that these pathways may result in the different mAb production between HP and LP. Secondly, only negligible changes occur in metabolic pathways at the early growth phase between HP and LP, whereas significant changes were found at the late growth phase. The most significantly up-regulated pathways during the late growth phase were related to oxidative phosphorylation, TCA cycle, and PPP. Taking all these pathway differences, with our observation, it was suggested that HP is more energetically efficient by directing glycolytic flux to the TCA cycle in conjunction with oxidative PPP to generate NADPH, which is consistent with the understandings from a previous study [50].

Since transcriptomics only infers metabolic pathway alternations from changes in gene expression, it can be misleading on reaction activity because of the possible complex post-transcriptional and metabolic regulatory [50]. Therefore, we conducted flux analysis using a genome-scale CHO model, with a focus on the metabolic reactions found in the transcriptomics analysis. Our analysis showed a positive correlation between predicted flux rates and transcriptional changes in many reactions. In contrast to this, several reactions revealed discrepancies between changes in gene expression and predicted fluxes, such as the reactions of G6PD, GPI, and TKT. These weak correlations indicate alternative regulatory mechanisms, such as post-transcriptional, post-translational, or allosteric control, which may require a more in-depth investigation for fundamental understanding. As metabolites represent the final outcome of combined gene expression and enzyme activities in the cells, the metabolome is considered as the ultimate read-out of cellular phenotype [56]. In this regard, the flux analysis generated from genome-scale models can also be integrated with intracellular metabolomics in the future, which allows to have a comprehensive exploration of the complex cell biology. The study performed by Yusufi et al. applied the metabolomics profiling to validate the predictions of genome-scale metabolic modeling, and revealed an increased level of metabolites that were involved in the energy-related metabolism and oxidative phosphorylation in protein-producing CHO cells [8].

Then, according to a comprehensive analysis of gene expression and flux distribution, we found several reactions and corresponding genes that can be of interest for future engineering targets. In the PPP, the fluxes predicted by the genome-scale model are higher in HP than LP during the late growth phase. But only the gene *PRPPS* shows higher expression in HP. One potential explanation for the discrepancy in gene expression levels and flux values for G6PD and TKT could involve post-transcriptional regulation and/or metabolic regulation; in contrast, the transcriptional regulation of gene *PRPPS* plays a leading role in reaction activity of PRPP synthesis. The metabolite PRPP is an important intermediate in cellular physiology. For example, it is utilized in the biosynthesis of nucleotides that are essential for building DNA and RNA; and it also served as a substrate for NAD generation which is an important redox factor [57,58]. Taken together, it is suggested that the reaction of PRPPS can be a very promising target to increase mAb productivity. Another interesting reaction is PDH where pyruvate is converted to acetyl-CoA, an important intermediate in the TCA cycle for energy production and lipid synthesis. Both gene expression and flux analyses pointed to a higher activity of PDH in HP, suggesting that the gene (e.g., the gene *Pdhb* which is one of DEGs in this study) in PDH can

be used as a marker for HP. In another recently published study, PDH was also recommended as markers for HPs and the enzyme to be metabolic targets as well [59]. After the identification of engineering targets, future work is to employ efficient genetic engineering tools to increase the activity of particular pathways. Taking the reactions of PRPPS and PDH as examples, we can focus on three candidate genes which have been identified as DEGs in transcriptomics analysis: genes *Prps1* (gene ID 100759532) and *Prps2* (Gene ID 100767893) from the reaction of PRPPS; gene *Pdhb* (gene ID 100774878) from the reaction of PDH. Genetic engineering strategies have widely applied in CHO cells, such as the successful applications of advanced gene editing CRISPR-Cas9 and transient expression techniques to improve cell growth or protein production in recent studies [60–62]. In each particular application of gene overexpression, either for a single gene or multiple genes, the effects on cell density, viability, and protein titer should be carefully assessed.

We also found that not all the reactions have higher activity in HP than LP in both gene expression and flux levels. It is interesting to note that the reactions of ODH and SUCOAS showed consistent trends between gene expression and flux prediction. The associated genes regulating ODH and SUCOAS are significantly expressed higher in HP cultures (the p-value was < 0.001 for gene *ODH* in comparison; the gene *SUCOAS* was identified as DEGs). More importantly, these two reactions are connected with amino acids metabolism, where a-ketoglutarate and succinyl-CoA are two crucial intermediates closely linked to amino acids [63]. One hypothesis could be that the HP cells have a higher ability to utilize the carbon backbones through the catabolism of amino acids for the formation of TCA cycle intermediates, which ultimately are to be used for energy generation. In a separate study, four amino acids at higher concentrations which are closely correlated to TCA cycle intermediates were supplemented in the feed and resulted in the higher activity of the TCA cycle according to metabolic pathway analysis, and increased mAb production compared to the control. This result was also confirmed by the measured oxygen uptake rate (OUR) (Huang et al., under review). However, it should also be noted that when the amino acids are supplied in excess, it will lead to the formation of inhibitory intermediates and harm mAb production [64,65]. Taken together, these two reactions can be potentially used as targets for media optimization through the modification of the amino acids associated with these two reactions. On the other hand, feeding TCA cycle intermediates such as a-ketoglutarate and succinate in the late exponential phase would be another potential strategy to improve the product titer. Coincidentally, a recent study conducted by Zhang et al. has demonstrated that feeding a-ketoglutarate, malate, and succinate in the stationary phase significantly improved cell specific productivity and antibody titer in CHO cells [66]. Additionally, the genes involved in ODH and SUCOAS can also be used as genetic targets for cell line development.

4. Conclusions

In this study, we aimed at using an integrated analysis to understand the intracellular metabolism change associated with mAb productivity. In our strategy, we started with using gene expression information to explore the metabolic alternations in response to batch conditions and different cell lines. The two-step comparison analysis orthogonally looking at the difference in the time course of mAb-producing culture process and the difference between high- and low- producing cells consistently revealed a series of high activity in metabolic pathways for high mAb production. We also integrated flux balance analysis in our approach to address the limitation in looking only at transcriptional alteration, for comparison with the metabolic changes in the pathways identified by transcriptomics analysis.

As our results are consistent with existing literature, for the first time, these key pathways are identified to be characteristics of high mAb production, not only for high-producing cell lines but also for a dynamic phenomenon in mAb-producing cell culture. And more importantly, these results are verified at both gene expression and metabolic flux level. After all, our study shows successful employment of multi-analysis combined strategy to comprehensively elucidate the metabolism in cell culture. Based on that, potential metabolic targets can be identified for future engineering considerations.

CRediT authorship contribution statement

Zhuangrong Huang: Conceptualization, Data curation, Formal analysis, Methodology, Visualization, Writing - original draft. **Seongkyu Yoon:** Funding acquisition, Investigation, Project administration, Resources, Software, Supervision, Validation, Writing - review & editing.

Declaration of Competing Interest

The authors declare that they have no known competing financial interests or personal relationships that could have appeared to influence the work reported in this paper.

Acknowledgments

We thank Dr. Seoyoung Park for supporting the lab work in LC–MS/MS. We are deeply grateful to Dr. Sha Sha for supporting the lab work in RNA-Seq, insightful discussions and valuable suggestions on the manuscript preparation. The study was supported by grants from NSF (1706731) and NSF/IUCRC AMBIC (1624718).

Appendix A. Supplementary data

Supplementary material related to this article can be found, in the online version, at doi:https://doi.org/10.1016/j.bej.2020.107624.

References

[1] G. Stolfa, M.T. Smonskey, R. Boniface, A.B. Hachmann, P. Gulde, A.D. Joshi, A.P. Pierce, S.J. Jacobia, A. Campbell, CHO-omics review: the impact of current and emerging technologies on Chinese hamster ovary based bioproduction, Biotechnol. J. 13 (2018) e1700227.
[2] C.A. Orellana, E. Marcellin, R.W. Palfreyman, T.P. Munro, P.P. Gray, L.K. Nielsen, RNA-seq highlights high clonal variation in monoclonal antibody producing CHO cells, Biotechnol. J. 13 (2018) e1700231.
[3] C.A. Orellana, E. Marcellin, B.L. Schulz, A.S. Nouwens, P.P. Gray, L.K. Nielsen, High-antibody-producing Chinese hamster ovary cells up-regulate intracellular protein transport and glutathione synthesis, J. Proteome Res. 14 (2015) 609–618.
[4] N. Romanova, T. Noll, Engineered and natural promoters and chromatin-modifying elements for recombinant protein expression in CHO cells, Biotechnol. J. 13 (2018) e1700232.
[5] A. Richelle, N.E. Lewis, Improvements in protein production in mammalian cells from targeted metabolic engineering, Curr. Opin. Syst. Biol. 6 (2017) 1–6.
[6] J. Xu, M.S. Rehmann, X. Xu, C. Huang, J. Tian, N.X. Qian, Z.J. Li, Improving titer while maintaining quality of final formulated drug substance via optimization of CHO cell culture conditions in low-iron chemically defined media, MAbs 10 (2018) 488–499.
[7] R.J. Graham, H. Bhatia, S. Yoon, Consequences of trace metal variability and supplementation on Chinese hamster ovary (CHO) cell culture performance: a review of key mechanisms and considerations, Biotechnol. Bioeng. 116 (2019) 3446–3456.
[8] F.N.K. Yusufi, M. Lakshmanan, Y.S. Ho, B.L.W. Loo, P. Ariyaratne, Y. Yang, S.K. Ng, T.R.M. Tan, H.C. Yeo, H.L. Lim, S.W. Ng, A.P. Hiu, C.P. Chow, C. Wan, S. Chen, G. Teo, G. Song, J.X. Chin, X. Ruan, K.W.K. Sung, W.S. Hu, M.G.S. Yap, M. Bardor, N. Nagarajan, D.Y. Lee, Mammalian systems biotechnology reveals global cellular adaptations in a recombinant CHO cell line, Cell Syst. 4 (2017) 530–542 e536.
[9] S. Sha, Z. Huang, Z. Wang, S. Yoon, Mechanistic modeling and applications for CHO cell culture development and production, Curr. Opin. Chem. Eng. 22 (2018) 54–61.
[10] C. Chen, H. Le, C.T. Goudar, Integration of systems biology in cell line and process development for biopharmaceutical manufacturing, Biochem. Eng. J. 107 (2016) 11–17.
[11] N. Xu, J. Ou, Y. Si, K.Y. Goh, D.D. Flanigan, X. Han, Y. Yang, S.-T. Yang, L. Zhou, X. Liu, Proteomics insight into the production of monoclonal antibody, Biochem. Eng. J. 145 (2019) 177–185.
[12] N.E. Lewis, X. Liu, Y. Li, H. Nagarajan, G. Yerganian, E. O'Brien, A. Bordbar, A.M. Roth, J. Rosenbloom, C. Bian, M. Xie, W. Chen, N. Li, D. Baycin-Hizal, H. Latif, J. Forster, M.J. Betenbaugh, I. Famili, X. Xu, J. Wang, B.O. Palsson, Genomic landscapes of Chinese hamster ovary cell lines as revealed by the Cricetulus griseus draft genome, Nat. Biotechnol. 31 (2013) 759–765.

[13] S. Sha, H. Bhatia, S. Yoon, An RNA-seq based transcriptomic investigation into the productivity and growth variants with Chinese hamster ovary cells, J. Biotechnol. 271 (2018) 37–46.
[14] A. Bedoya-Lopez, K. Estrada, A. Sanchez-Flores, O.T. Ramirez, C. Altamirano, L. Segovia, J. Miranda-Rios, M.A. Trujillo-Roldan, N.A. Valdez-Cruz, Effect of temperature downshift on the transcriptomic responses of Chinese Hamster ovary cells using recombinant human tissue plasminogen activator production culture, PLoS One 11 (2016) e0151529.
[15] D. Fomina-Yadlin, M. Mujacic, K. Maggiora, G. Quesnell, R. Saleem, J.T. McGrew, Transcriptome analysis of a CHO cell line expressing a recombinant therapeutic protein treated with inducers of protein expression, J. Biotechnol. 212 (2015) 106–115.
[16] E. Baek, J.S. Lee, G.M. Lee, Untangling the mechanism of 3-methyladenine in enhancing the specific productivity: transcriptome analysis of recombinant Chinese hamster ovary cells treated with 3-methyladenine, Biotechnol. Bioeng. 115 (2018) 2243–2254.
[17] A. Kantardjieff, N.M. Jacob, J.C. Yee, E. Epstein, Y.J. Kok, R. Philp, M. Betenbaugh, W.S. Hu, Transcriptome and proteome analysis of Chinese hamster ovary cells under low temperature and butyrate treatment, J. Biotechnol. 145 (2010) 143–159.
[18] T. Carlage, M. Hincapie, L. Zang, Y. Lyubarskaya, H. Madden, R. Mhatre, W.S. Hancock, Proteomic profiling of a high-producing Chinese Hamster ovary cell culture, Anal. Chem. 81 (2009) 7352–7362.
[19] W.P. Chong, S.H. Thng, A.P. Hiu, D.Y. Lee, E.C. Chan, Y.S. Ho, LC-MS-based metabolic characterization of high monoclonal antibody-producing Chinese hamster ovary cells, Biotechnol. Bioeng. 109 (2012) 3103–3111.
[20] R. Van Assche, V. Broeckx, K. Boonen, E. Maes, W. De Haes, L. Schoofs, L. Temmerman, Integrating-Omics: Systems biology as explored through C. Elegans research, J. Mol. Biol. 427 (2015) 3441–3451.
[21] D. Baycin-Hizal, D.L. Tabb, R. Chaerkady, L. Chen, N.E. Lewis, H. Nagarajan, V. Sarkaria, A. Kumar, D. Wolozny, J. Colao, E. Jacobson, Y. Tian, R.N. O'Meally, S.S. Krag, R.N. Cole, B.O. Palsson, H. Zhang, M. Betenbaugh, Proteomic analysis of Chinese hamster ovary cells, J. Proteome Res. 11 (2012) 5265–5276.
[22] Y. Gao, S. Ray, S. Dai, A.R. Ivanov, N.R. Abu-Absi, A.M. Lewis, Z. Huang, Z. Xing, M.C. Borys, Z.J. Li, B.L. Karger, Combined metabolomics and proteomics reveals hypoxia as a cause of lower productivity on scale-up to a 5000-liter CHO bioprocess, Biotechnol. J. 11 (2016) 1190–1200.
[23] H. Hefzi, K.S. Ang, M. Hanscho, A. Bordbar, D. Ruckerbauer, M. Lakshmanan, C.A. Orellana, D. Baycin-Hizal, Y. Huang, D. Ley, V.S. Martinez, S. Kyriakopoulos, N.E. Jimenez, D.C. Zielinski, L.E. Quek, T. Wulff, J. Arnsdorf, S. Li, J.S. Lee, G. Paglia, N. Loira, P.N. Spahn, L.E. Pedersen, J.M. Gutierrez, Z.A. King, A.M. Lund, H. Nagarajan, A. Thomas, A.M. Abdel-Haleem, J. Zanghellini, H.F. Kildegaard, B.G. Voldborg, Z.P. Gerdtzen, M.J. Betenbaugh, B.O. Palsson, M.R. Andersen, L.K. Nielsen, N. Borth, D.Y. Lee, N.E. Lewis, A consensus genome-scale reconstruction of Chinese hamster ovary cell metabolism, Cell Syst. 3 (2016) 434–443 e438.
[24] M. Lakshmanan, Y.J. Kok, A.P. Lee, S. Kyriakopoulos, H.L. Lim, G. Teo, S.L. Poh, W.Q. Tang, J. Hong, A.H. Tan, X. Bi, Y.S. Ho, P. Zhang, S.K. Ng, D.Y. Lee, Multi-omics profiling of CHO parental hosts reveals cell line-specific variations in bioprocessing traits, Biotechnol. Bioeng. 116 (2019) 2117–2129.
[25] M. Vodopivec, L. Lah, M. Narat, T. Curk, Metabolomic profiling of CHO fed-batch growth phases at 10, 100, and 1,000 L, Biotechnol. Bioeng. 116 (2019) 2720–2729.
[26] C. Chen, H. Le, B. Follstad, C.T. Goudar, A comparative transcriptomics workflow for analyzing microarray data from CHO cell cultures, Biotechnol. J. 13 (2018) e1700228.
[27] Z. Fang, R. Du, X. Cui, Uniform approximation is more appropriate for Wilcoxon Rank-Sum Test in gene set analysis, PLoS One 7 (2012) e31505.
[28] S.A. Kuyuk, I. Ercan, Commonly used statistical methods for detecting differential gene expression in microarray experiments, Biostat. Epidemiol. Int. J. (2017) 1–8.
[29] M. Maniruzzaman, M. Jahanur Rahman, B. Ahammed, M.M. Abedin, H.S. Suri, M. Biswas, A. El-Baz, P. Bangeas, G. Tsoulfas, J.S. Suri, Statistical characterization and classification of colon microarray gene expression data using multiple machine learning paradigms, Comput. Methods Programs Biomed. 176 (2019) 173–193.
[30] T. Mou, W. Deng, F. Gu, Y. Pawitan, T.N. Vu, Reproducibility of methods to detect differentially expressed genes from single-cell RNA sequencing, Front. Genet. 10 (2019) 1331.
[31] S. Park, Development and Application Metabolomics Approach for Understanding and Characterizing Mammalian Cells, Order No. 10970655 University of Massachusetts Lowell, 2018.
[32] F.C. Courtes, J. Lin, H.L. Lim, S.W. Ng, N.S. Wong, G. Koh, L. Vardy, M.G. Yap, B. Loo, D.Y. Lee, Translatome analysis of CHO cells to identify key growth genes, J. Biotechnol. 167 (2013) 215–224.
[33] C. Chen, H. Le, C.T. Goudar, An automated RNA-Seq analysis pipeline to identify and visualize differentially expressed genes and pathways in CHO cells, Biotechnol. Prog. 31 (2015) 1150–1162.
[34] W. Sommeregger, P. Mayrhofer, W. Steinfellner, D. Reinhart, M. Henry, M. Clynes, P. Meleady, R. Kunert, Proteomic differences in recombinant CHO cells producing two similar antibody fragments, Biotechnol. Bioeng. 113 (2016) 1902–1912.
[35] C. Xie, X. Mao, J. Huang, Y. Ding, J. Wu, S. Dong, L. Kong, G. Gao, C.Y. Li, L. Wei, KOBAS 2.0: a web server for annotation and identification of enriched pathways and diseases, Nucleic Acids Res. 39 (2011) W316–322.
[36] X. Mao, T. Cai, J.G. Olyarchuk, L. Wei, Automated genome annotation and pathway identification using the KEGG Orthology (KO) as a controlled vocabulary, Bioinformatics 21 (2005) 3787–3793.
[37] Y.H. Shi, S.W. Zhu, X.Z. Mao, J.X. Feng, Y.M. Qin, L. Zhang, J. Cheng, L.P. Wei, Z.Y. Wang, Y.X. Zhu, Transcriptome profiling, molecular biological, and physiological studies reveal a major role for ethylene in cotton fiber cell elongation, Plant Cell 18 (2006) 651–664.
[38] C. Li, X. Li, Y. Miao, Q. Wang, W. Jiang, C. Xu, J. Li, J. Han, F. Zhang, B. Gong, L. Xu, SubpathwayMiner: a software package for flexible identification of pathways, Nucleic Acids Res. 37 (2009) e131.
[39] P.C. Li, S.W. Yu, K. Li, J.G. Huang, X.J. Wang, C.C. Zheng, The mutation of glu at amino acid 3838 of AtMDN1 provokes pleiotropic developmental phenotypes in Arabidopsis, Sci. Rep. 6 (2016) 36446.
[40] Y. Benjamini, Y. Hochberg, Controlling the false discovery rate a practical and powerful approach to multiple testing, J. R. Stat. Soc. Ser. B 57 (1995) 289–300.
[41] Z. Huang, D.Y. Lee, S. Yoon, Quantitative intracellular flux modeling and applications in biotherapeutic development and production using CHO cell cultures, Biotechnol. Bioeng. 114 (2017) 2717–2728.
[42] L.E. Quek, S. Dietmair, J.O. Kromer, L.K. Nielsen, Metabolic flux analysis in mammalian cell culture, Metab. Eng. 12 (2010) 161–171.
[43] J.D. Orth, I. Thiele, B.O. Palsson, What is flux balance analysis? Nat. Biotechnol. 28 (2010) 245–248.
[44] N.E. Lewis, K.K. Hixson, T.M. Conrad, J.A. Lerman, P. Charusanti, A.D. Polpitiya, J.N. Adkins, G. Schramm, S.O. Purvine, D. Lopez-Ferrer, K.K. Weitz, R. Eils, R. Konig, R.D. Smith, B.O. Palsson, Omic data from evolved E. coli are consistent with computed optimal growth from genome-scale models, Mol. Syst. Biol. 6 (2010) 390.
[45] C. Calmels, A. McCann, L. Malphettes, M.R. Andersen, Application of a curated genome-scale metabolic model of CHO DG44 to an industrial fed-batch process, Metab. Eng. 51 (2019) 9–19.
[46] S.A. Becker, A.M. Feist, M.L. Mo, G. Hannum, B.O. Palsson, M.J. Herrgard, Quantitative prediction of cellular metabolism with constraint-based models: the COBRA Toolbox, Nat. Protoc. 2 (2007) 727–738.
[47] J. Schellenberger, R. Que, R.M. Fleming, I. Thiele, J.D. Orth, A.M. Feist, D.C. Zielinski, A. Bordbar, N.E. Lewis, S. Rahmanian, J. Kang, D.R. Hyduke, B.O. Palsson, Quantitative prediction of cellular metabolism with constraint-based models: the COBRA Toolbox v2.0, Nat. Protoc. 6 (2011) 1290–1307.
[48] N. Templeton, J. Dean, P. Reddy, J.D. Young, Peak antibody production is associated with increased oxidative metabolism in an industrially relevant fed-batch CHO cell culture, Biotechnol. Bioeng. 110 (2013) 2013–2024.
[49] W.S. Ahn, M.R. Antoniewicz, Metabolic flux analysis of CHO cells at growth and non-growth phases using isotopic tracers and mass spectrometry, Metab. Eng. 13 (2011) 598–609.
[50] N. Templeton, K.D. Smith, A.G. McAtee-Pereira, H. Dorai, M.J. Betenbaugh, S.E. Lang, J.D. Young, Application of (13)C flux analysis to identify high-productivity CHO metabolic phenotypes, Metab. Eng. 43 (2017) 218–225.
[51] M. Yang, K.H. Vousden, Serine and one-carbon metabolism in cancer, Nat. Rev. Cancer 16 (2016) 650–662.
[52] D. Christodoulou, H. Link, T. Fuhrer, K. Kochanowski, L. Gerosa, U. Sauer, Reserve flux capacity in the pentose phosphate pathway enables Escherichia coli's rapid response to oxidative stress, Cell Syst. 6 (2018) 569–578 e567.
[53] A.M. Davy, H.F. Kildegaard, M.R. Andersen, Cell factory engineering, Cell Syst. 4 (2017) 262–275.
[54] V.S. Martinez, S. Dietmair, L.E. Quek, M.P. Hodson, P. Gray, L.K. Nielsen, Flux balance analysis of CHO cells before and after a metabolic switch from lactate production to consumption, Biotechnol. Bioeng. 110 (2013) 660–666.
[55] N. Dhami, D.K. Trivedi, R. Goodacre, D. Mainwaring, D.P. Humphreys, Mitochondrial aconitase is a key regulator of energy production for growth and protein expression in Chinese hamster ovary cells, Metabolomics 14 (2018) 136.
[56] H.F. Kildegaard, D. Baycin-Hizal, N.E. Lewis, M.J. Betenbaugh, The emerging CHO systems biology era: harnessing the' omics revolution for biotechnology, Curr. Opin. Biotechnol. 24 (2013) 1102–1107.
[57] B. Hove-Jensen, K.R. Andersen, M. Kilstrup, J. Martinussen, R.L. Switzer, M. Willemoës, Phosphoribosyl Diphosphate (PRPP): biosynthesis, enzymology, utilization, and metabolic significance, Microbiol. Mol. Biol. Rev. 81 (2017) e00040–00016.
[58] A. Chiarugi, C. Dolle, R. Felici, M. Ziegler, The NAD metabolome – a key determinant of cancer cell biology, Nat. Rev. Cancer 12 (2012) 741–752.
[59] C. Calmels, S. Arnoult, B. Ben Yahia, L. Malphettes, M.R. Andersen, Application of a genome-scale model in tandem with enzyme assays for identification of metabolic signatures of high and low CHO cell producers, Metab. Eng. Commun. (2019) e00097.
[60] C.A. Orellana, E. Marcellin, P.P. Gray, L.K. Nielsen, Overexpression of the regulatory subunit of glutamate-cysteine ligase enhances monoclonal antibody production in CHO cells, Biotechnol. Bioeng. 114 (2017) 1825–1836.
[61] D. Ley, S. Pereira, L.E. Pedersen, J. Arnsdorf, H. Hefzi, A.M. Davy, T.K. Ha, T. Wulff, H.F. Kildegaard, M.R. Andersen, Reprogramming AA catabolism in CHO cells with CRISPR/Cas9 genome editing improves cell growth and reduces byproduct secretion, Metab. Eng. 56 (2019) 120–129.
[62] A. Berger, V. Le Fourn, J. Masternak, A. Regamey, I. Bodenmann, P.-A. Girod, N. Mermod, Overexpression of transcription factor Foxa1 and target genes remediate therapeutic protein production bottlenecks in Chinese hamster ovary cells, Biotechnol. Bioeng. 117 (2020) 1101–1116.
[63] S. Pereira, H.F. Kildegaard, M.R. Andersen, Impact of CHO metabolism on cell growth and protein production: an overview of toxic and inhibiting metabolites and nutrients, Biotechnol. J. 13 (2018) e1700499.
[64] B.C. Mulukutla, J. Kale, T. Kalomeris, M. Jacobs, G.W. Hiller, Identification and control of novel growth inhibitors in fed-batch cultures of Chinese hamster ovary cells, Biotechnol. Bioeng. 114 (2017) 1779–1790.
[65] B.C. Mulukutla, J. Mitchell, P. Geoffroy, C. Harrington, M. Krishnan, T. Kalomeris, C. Morris, L. Zhang, P. Pegman, G.W. Hiller, Metabolic engineering of Chinese hamster ovary cells towards reduced biosynthesis and accumulation of novel growth inhibitors in fed-batch cultures, Metab. Eng. 54 (2019) 54–68.
[66] X. Zhang, R. Jiang, H. Lin, S. Xu, Feeding tricarboxylic acid cycle intermediates improves lactate consumption and antibody production in Chinese hamster ovary cell cultures, Biotechnol. Progr. (2020) e2975.